

# Relative Intensity Correction of Raman Spectrometers: NIST SRMs 2241 Through 2243 for 785 nm, 532 nm, and 488 nm/514.5 nm Excitation

STEVEN J. CHOQUETTE,\* EDGAR S. ETZ, WILBUR S. HURST,  
DOUGLAS H. BLACKBURN, and STEFAN D. LEIGH

*Chemical Science and Technology Laboratory, National Institute of Standards and Technology, Gaithersburg, Maryland 20899-8394*

Standard Reference Materials® SRMs 2241 through 2243 are certified spectroscopic standards intended for the correction of the relative intensity of Raman spectra obtained with instruments employing laser excitation wavelengths of 785 nm, 532 nm, or 488 nm/514.5 nm. These SRMs each consist of an optical glass that emits a broadband luminescence spectrum when illuminated with the Raman excitation laser. The shape of the luminescence spectrum is described by a polynomial expression that relates the relative spectral intensity to the Raman shift with units in wavenumber ( $\text{cm}^{-1}$ ). This polynomial, together with a measurement of the luminescence spectrum of the standard, can be used to determine the spectral intensity-response correction, which is unique to each Raman system. The resulting instrument intensity-response correction may then be used to obtain Raman spectra that are corrected for a number of, but not all, instrument-dependent artifacts. Peak area ratios of the intensity-corrected Raman spectrum of cyclohexane are presented as an example of a methodology to validate the spectral intensity calibration process and to illustrate variations that can occur in this measurement.

Index Headings: Standard Reference Material®; Raman intensity standard; Intensity calibration; Optical filters; Raman spectroscopy; Luminescence; Intensity correction; Spectral irradiance.

## INTRODUCTION

Historically, spectra obtained using dispersive Raman spectrometers with laser excitation in the visible or the near-infrared regions generally have not been corrected for the instrumental response. Raman spectra obtained with different instruments may show significant variations in the measured relative peak intensities, mainly as a result of differences in their wavelength-dependent optical transmission and in their detector quantum efficiency. These variations can be particularly large when widely different laser excitations are used, but can occur even when the same laser excitation is used. In methods to correct the response, generally the issue to be addressed is the manner in which to employ a source of known relative irradiance, since most users are not attempting to obtain spectra characterized by absolute Raman intensities.

Raman intensity calibration based upon white-light calibra-

tion lamps, whose spectral output often is calibrated relative to a NIST or another National Metrology Institute (NMI)-traceable irradiance source, provides one method for determination of the corrections. Such lamps have a defined spectral output of intensity versus wavelength and have been used by several groups to calibrate the spectral response of Raman spectrometers.<sup>1-4</sup> However, intensity calibration using a white-light source can present experimental difficulties that are not easily dealt with in routine analytical work.<sup>1,5</sup> Calibrated standard tungsten lamps or, tungsten-halogen lamps that are now in common use for spectroscopy, have a limited lifetime and require periodic recalibration. Tungsten-halogen lamps are often mounted into an integrating sphere to eliminate polarization effects and to provide uniform source irradiance. In practice, these irradiance sources can be difficult to interface with the variety of sampling arrangements that are common now with typical Raman spectrometers.

Secondary emission standards, in the form of materials that are luminescent with laser irradiation, can be calibrated to provide a source of known relative irradiance. Several investigators have proposed this approach for both Raman and fluorescence spectroscopy.<sup>6-9</sup> This approach has the advantages that it is easy to use on a daily basis with any sampling configuration, requires no additional instrumentation, and does not require expensive periodic recalibration of the irradiance source. An additional advantage is that, with proper positioning of the emission standard, the luminescence generated by the laser source retraces the Raman optical sampling path.

In cooperation with the ASTM Subcommittee on Raman Spectroscopy (E13.08), the National Institute of Standards and Technology (NIST) has been developing a suite of glasses that are luminescent with the visible laser radiation wavelengths that are in common use by the Raman community. The goal of this work has been to provide secondary emission standards for routine calibration of the intensity response of Raman spectrometers that are acceptable for use in a variety of analytical settings. Practical concerns have meant that these standards should be in solid, not liquid, form.

Today's applications of Raman spectroscopy often require analytical method transfer, transportability of user-generated spectral libraries, and performance validation. Intensity cali-

Received 19 September 2006; accepted 28 November 2006.

\* Author to whom correspondence should be sent. E-mail: steven.choquette@nist.gov.

bration will make these procedures more robust and instrument-independent and will aid in the use of Raman spectra for quantitation. Therefore, it is reasonable to expect that Raman relative intensity calibration will become a requirement in a number of analytical applications. With the proliferation of portable Raman spectrometers, it is anticipated that the need for fast, easy-to-use and repeatable calibration in the field will be required.

This paper describes the development and calibration of three NIST Standard Reference Materials (SRMs®). These luminescent glass standards are designed for the relative intensity calibration of Raman spectrometers operating with 785 nm, 532 nm, or 488 nm/514.5 nm laser excitation.<sup>10</sup> These secondary emission standards may be used for the routine calibration of the intensity of Stokes shifted Raman spectra obtained at these laser excitation wavelengths. Work is in progress on at least one other standard for use with Raman excitation at 1064 nm. In addition, results are presented for the measurement of intensity-corrected peak area ratios of the spectrum of cyclohexane obtained from typical Raman systems. These results have implications for protocols in methods that use peak-area ratio measurements to validate the intensity-correction procedure.

## EXPERIMENTAL METHODS

An experimental design was implemented to identify and minimize systematic effects that affect the measurement of the intensity-corrected luminescence spectra of the SRM glasses. The factors that were varied included measurements with three Raman spectrometer systems, the use of two uniform integrating spheres as sources of known relative irradiance, a variety of sampling optics, and changes in the laser-beam parameters that varied from point focus, line focus, and collimated (unfocused) beams. Studies of the dependence of the luminescent shape on the temperature of the SRM glasses and on the wavelength of excitation were also performed.

## SPECTROMETER SYSTEMS

**Micro-Raman System.** One of the spectrometer systems utilized for the certification of these glasses was a model S1000 micro-Raman system manufactured by Renishaw (Hoffman Estates, Ill).<sup>†</sup> This instrument consists of a 250 mm focal length imaging spectrometer with both 1200 and 1800 grooves/mm holographic gratings and is coupled to an Olympus BH-2 microscope. This system has a proprietary 12.5 mm wide deep-depletion charge-coupled device (CCD) detector array format of 250 (row) by 577 (column) pixels, with enhanced sensitivity in the near-infrared region (NIR, 750 to 1050 nm). For the purposes of certification of the SRM glasses, a spectrometer slit width of 30  $\mu\text{m}$  was used and only the central 20 to 30 rows of the CCD were binned to collect the spectrum. The spectral resolution was 3  $\text{cm}^{-1}$  or better (as determined from the full-width at half-maximum (FWHM) of a neon emission line) and the instrumental reproducibility was approximately  $\pm 1 \text{ cm}^{-1}$ , for measurements with 785 nm excitation. A 25 mm diameter polarization scrambler (Optics for Research, model DPU-25,

Caldwell, NJ) was inserted into the collimated beam portion of the emission to depolarize both the luminescence and the Raman scattered light. All spectra were acquired in the continuous scanning mode of the instrument.

**Macro-Raman Systems.** The other Raman systems used in this study were macro-Raman systems and consisted of either a model HR460 imaging spectrometer made by JY Horiba (Edison, NJ) or two different models of 500-i imaging spectrometer made by Princeton Instruments/Acton Corporation (Princeton, NJ). The JY Horiba spectrometer had a 460 mm focal length, an  $f/5.3$  aperture, and two 1200 grooves/mm gratings blazed at 630 nm or 500 nm and a 600 grooves/mm holographic grating blazed at 500 nm. Back-illuminated CCD detectors were always used with this spectrometer and for the majority of the data the CCD had 24  $\mu\text{m}$  square pixels in an array of 1100 columns by 330 rows. The Acton spectrometers had a 500 mm focal length, an  $f/6.5$  aperture, and a ruled 1200 grooves/mm grating that was blazed at 500 nm. The Acton spectrometers were equipped with back-illuminated CCDs, with a format of either 2048 columns by 512 rows of pixels with dimensions of 13.5  $\mu\text{m} \times 13.5 \mu\text{m}$  or a format of 1340 columns by 400 rows with dimensions of 20  $\mu\text{m}$  square pixels. Etaloning effects on the signal obtained from these back-illuminated CCDs were easily apparent at wavelengths greater than approximately 900 nm and were usually 5% to 10% of the signal (peak-to-peak variation); however, for one CCD it was as large as 30%. For all spectrometers, the spectral instrumental bandpass (FWHM) was less than  $\sim 4 \text{ cm}^{-1}$  and the instrumental reproducibility was approximately  $\pm 2 \text{ cm}^{-1}$  over the range of wavelengths covered. All measurements were made with a spectrometer slit width of 100  $\mu\text{m}$ .

A schematic of the collection optics for the measurements with the JY Horiba or the Acton spectrometers is shown in Fig. 1. Over the course of the measurements, visible-range achromatic collection lenses (design wavelengths of 486.1 nm, 587.6 nm, and 656.3 nm) with focal lengths of 160 mm and 200 mm were used. In the collimated light path, holographic notch filters (Kaiser Optical Systems Supernotch-Plus, Ann Arbor, MI), matched to the appropriate excitation laser wavelength, with a spectral bandwidth of 10 nm and an out-of-band optical density greater than 6.0, were used to block the Rayleigh scattered light from entering the spectrometer. This was followed by a 25 mm diameter polarization scrambler (Optics for Research, model DPU-25, Caldwell, NJ) to depolarize both the luminescence and the Raman scattered light. Lastly, long-pass filters were placed just before the focusing lens (and in the collimated light path) to prevent second-order diffracted light from the grating from making false spectral contributions. The visible-range achromatic focusing lenses used at various times were of 160 mm, 300 mm, or 350 mm focal length, which either just slightly or easily under-filled the grating, to minimize stray scattered light within the spectrometer. Samples were held on a sample stage that had micrometer adjustments in the x and y horizontal plane and screw-type vertical adjustment.

Raman, glass luminescence, and white light spectra were always obtained in the 180° backscattering configuration. Most measurements were made using a 300 mm focal length cylindrical lens to form a line focus of the laser beam on the sample, with beam dimensions on the sample of approximately 80  $\mu\text{m}$  wide by 4 mm high. In addition, measurements were also made with a 300 mm spherical lens that focused the beam

<sup>†</sup> Certain commercial equipment, instruments, or materials are identified in this document. Such identification does not imply recommendation or endorsement by the National Institute of Standards and Technology, nor does it imply that the products identified are necessarily the best available for the purpose.

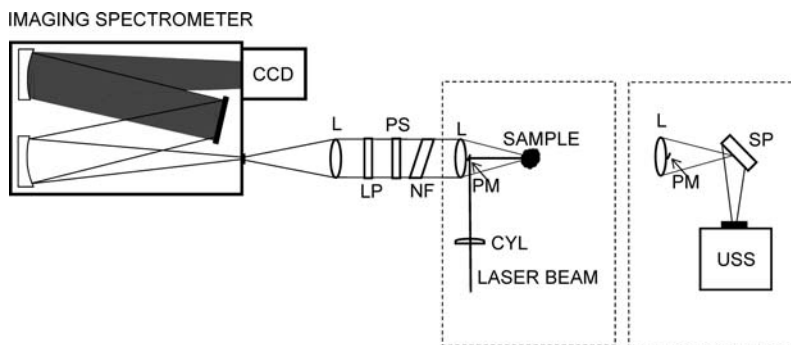


FIG. 1. Optical layout of the JY HORIBA and Acton spectrometer systems. Options are shown for collection of white light and Raman spectra. L = achromatic lens, LP = long-pass filter, PS = polarization scrambler, NF = notch filter, PM = pickoff mirror, CYL = cylindrical singlet lens, SP = Spectralon, and USS = uniform sphere source.

to an approximately 80  $\mu\text{m}$  diameter spot on the sample and with an unfocused beam that used no focusing lens and resulted in approximately a 2 mm diameter spot on the sample. A 4 mm square pickoff mirror was placed just in front of the collection lens to direct the laser beam onto the sample.

In work with the macro-Raman systems, variations in the measured shapes of the luminescence spectra were observed as the position of the glass sample surface relative to the focus point of the collection lens was changed. For this reason, close attention was given to the location of the focal point of the collection optic relative to the front surface of the glass sample. A photographic microscope resolution chart was mounted inside a 1 mm path length cuvette and was placed at the sample position for focusing. After a number of independent determinations, it was judged that the focus point of the collection lens could be determined to  $\pm 0.5$  mm.

**Excitation Lasers.** The same 785 nm and 532 nm lasers were used for measurements with the three spectrometer systems. The 785 nm excitation was obtained from a Coherent model 90-5 argon ion laser (5 W) that optically pumped a Coherent (Sunnyvale, CA) model 890 Titanium Sapphire (Ti:S) laser. A holographic laser bandpass filter (Kaiser Optical) was used to block the laser plasma lines. The Ti:S laser was adjusted to operate at wavelengths between 784.9 nm to 785.1 nm for the certification measurements of SRM 2241. The 532 nm excitation was obtained from a 200 mW model 142 diode pumped single-frequency Nd:YAG continuous wave laser manufactured by Lightwave Electronics (Mountain View, CA). Its wavelength was measured to be 532.199 nm for the duration of the certification period (>12 months) with a Coherent Wavemaster™ wavemeter.

Different argon ion gas lasers were optically coupled to each of the spectrometers for 488 nm and 514.5 nm excitation for certification of SRM 2243. Again, holographic band pass filters were used to block the laser plasma lines. The Raman shift was calculated using laser wavelengths taken as 487.9860 nm and 514.5319 nm.

## SPECTROMETER CALIBRATION

**Calibration of the Intensity Axis.** Two NIST calibrated sources of white-light irradiance were used during the course of these certification measurements. Both were six-inch uniform sphere sources (Model # US-60-SL, Labsphere, Nashua, NH) with Spectralon interior reflecting surfaces and equipped with internally mounted 10 W quartz tungsten halogen lamps. These

spheres were modified with an internal light baffle so that direct radiation from the lamp could not exit the spheres and an iris diaphragm was added to the exit. For clarity, these integrating sphere sources will be henceforth referred to as  $LS_1$  and  $LS_2$ . Both spheres were run in constant current mode. These spheres were calibrated for their relative spectral irradiance by the Optical Technology Division at NIST.<sup>11</sup> The calibration units of the irradiance are given as  $\text{Watt}/(\text{cm}^2 \text{ nm})$ . These units must be converted to  $\text{photons s}^{-1} \text{ cm}^{-2} (\text{cm}^{-1})^{-1}$  for use in Raman spectrometers with CCD detectors that are photon-counting devices, where the wavenumber unit ( $\text{cm}^{-1}$ ) is the reciprocal of the wavelength expressed in centimeters. The unit Watt is converted to the number of photons  $n$ , by multiplying by  $\lambda$ , from the Planck relation  $n = E\lambda/hc$ .  $E$  is the energy in watts,  $\lambda$  is the wavelength in nm,  $h$  is Planck's constant (J s), and  $c$  is the speed of light ( $\text{m s}^{-1}$ ). Conversion from the wavelength scale to the wavenumber scale requires multiplication by an additional factor of  $\lambda^2$ , since the physical expression for the measured irradiance is an integral equation ( $-\delta\nu = 1/\lambda^2 \delta\lambda$ ).<sup>12</sup> After conversion of units to the absolute wavenumber scale, the irradiance scale is then transformed to a scale of Raman shift from a given laser excitation wavelength.

The spectral range of calibration of each of the two light sources,  $LS_x$ , spans from 400 nm to 1200 nm, with 20 nm spacing, and from 1225 nm to 1800 nm, with 25 nm spacing. Polynomials were fitted to sub-ranges of this calibration data to provide a parametric model for the known spectral irradiance. Defining  $I_{LS_x}$  as the spectral irradiance of either  $LS_1$  or  $LS_2$ ,  $I_{LS_x}$  is the polynomial for a given wavelength sub-range:

$$I_{LS_x}(\Delta\nu) = A_0 + A_1 \times (\Delta\nu)^1 + A_2 \times (\Delta\nu)^2 + \dots + A_n \times (\Delta\nu)^n \quad (1)$$

where  $\Delta\nu$  is the data point spacing in Raman shift ( $\text{cm}^{-1}$ ).

For a measurement of the intensity of either  $LS_1$  or  $LS_2$  by a spectrometer system, the spectrally distributed quantity

$$C_{LS_x} = (I_{LS_x})/S_{LS_x} \quad (2)$$

where  $S_{LS_x}$  is the measured intensity of the  $LS_x$  source, should be independent of the source used. These quantities,  $C_{LS_x}$ , form a set of relative intensity correction factors we term the spectral intensity correction curve. It is independent of the irradiance source for a given instrument, but will be unique for each

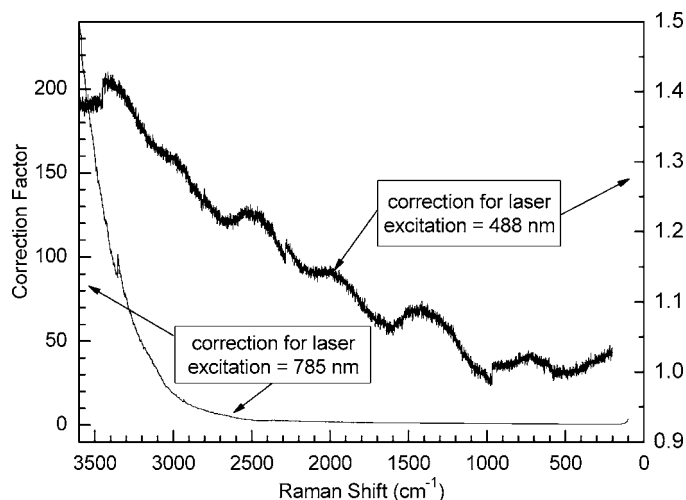


FIG. 2. Sample relative intensity correction curves for the JY HORIBA Raman system with 785 nm and 488 nm excitation.

instrument and set of collection conditions. Using

$$\Delta = \left[ \left( C_{LS2(\lambda)} - C_{LS1(\lambda)} \right) \right] / C_{LS2(\lambda)}$$

where  $C_{LSx}$  is the correction factor, for both the Renishaw and the macro-Raman systems, there was less than  $\Delta = 2\%$  difference over the entire range of spectral calibration ( $200 \text{ cm}^{-1}$  to  $3600 \text{ cm}^{-1}$  or  $4000 \text{ cm}^{-1}$ ) for all of the wavelength sub-ranges. As a result, both  $LS_1$  and  $LS_2$  sources were used as independent irradiance sources for the certification of the luminescent spectra of the SRM glasses.

Examples of intensity correction curves obtained with one of the macro-Raman systems are illustrated in Fig. 2. The large numerical range of the correction factors for Raman systems with laser excitation at 785 nm mostly results from the onset of a substantial decrease in CCD photon sensitivity that starts at approximately  $1000 \text{ nm}$  ( $\sim 3000 \text{ cm}^{-1}$  Raman shift), as the wavelength approaches the band-edge of silicon. The much smaller changes, shown for Raman shifts for laser excitation at 488 nm, are typical of what is observed for most systems with lasers operating between 488 nm and 632 nm.

For the measurement of the white light spectrum, the sphere source was aligned to the optical axis of the Renishaw spectrometer using the excitation laser and a  $200 \mu\text{m}$  pinhole placed on the microscope sampling stage in the focal plane of the microscope objective. The pinhole was visually aligned to be in the center of the field of view and then the (highly attenuated) laser beam was focused through the pinhole. Adjustments were made to the x and y positions of the pinhole until the laser passed through the pinhole with a minimum of attenuation and vignetting. The sphere source was placed 10 cm from the base of the microscope, with its output optical axis parallel to the optical table, which is perpendicular to the spectrometer optical axis. The sphere source light was scattered upward onto the pinhole with a 1 in. diameter piece of Spectralon placed at  $45^\circ$  to the optic axis of the spectrometer. All calibration spectra were acquired from the white light emerging from the pinhole. Separate calibration spectra were acquired for each objective lens used ( $10\times$  NA 0.25,  $20\times$  NA 0.4).

The macro-Raman systems were calibrated with the

experimental arrangement as illustrated in Fig. 1. A 50 mm diameter piece of Spectralon was placed at the sample position at an angle of 45 degrees to the optical axis to the spectrometer. The sphere source was placed at 90 degrees to this optical axis and extra light baffling was added to ensure that only white light reflecting off the Spectralon mounted in the sample position was collected.

**Calibration of Wavelength Axis.** Wavelength calibration (x-axis) of the spectrometers was performed with a neon pen lamp.<sup>13</sup> All three instruments were calibrated in absolute  $\text{cm}^{-1}$  (air) for the appropriate Raman spectral region, i.e., from  $200 \text{ cm}^{-1}$  to  $3600 \text{ cm}^{-1}$  Raman shift from the excitation wavelength. For 785 nm and 532 nm laser excitation, the laser wavelength was determined with a Coherent wavemeter. The Raman shift ( $\text{cm}^{-1}$ ) axis, relative to this laser line, was checked by measuring the Raman shift position of the silicon phonon ( $520 \text{ cm}^{-1}$ ) and also the spectrum of a number of Raman shift standards proposed by the ASTM.<sup>14</sup>

**Treatment of Data.** All spectra were background subtracted. After conversion of units to the absolute wavenumber scale, the spectra are then transformed to a scale of Raman shift from a given laser excitation wavenumber.

The intensity-corrected spectrum is obtained by multiplying the intensity correction factor by the intensity of the measured luminescence of the SRM:

$$S_{\text{CORR SRM}}(\Delta\nu) = C_{LSx}(\Delta\nu) \times S_{\text{MEAS SRM}}(\Delta\nu) \quad (3)$$

The construction of the spectrometer spectral correction curve,  $S_{\text{CORR SRM}}(\Delta\nu)$ , and the conversion of the measured sample spectrum to a corrected spectrum used a combination of in-house programs and proprietary commercial software. Intensity-corrected luminescence or Raman data were then obtained using Galactic Grams32 (Thermo-Electron Corp, Nashua, NH) by multiplying the spectral data point by point with the white-light spectral correction curve.

**Fabrication of Luminescent Glasses.** In considering various glasses as candidates for Raman intensity standards, a number of requirements must be met. Their spectra must consist of a broad-band luminescence that spans the relevant Raman shift region ( $200 \text{ cm}^{-1}$  to  $4000 \text{ cm}^{-1}$ ), must display a smoothly varying shape with a lack of vibronic features in this spectrum, should be photostable, must possess a suitable level of luminescence, and must have very low absorbance of the excitation laser to prevent heating. Various glass matrices doped with luminescent metal ions were investigated to find glasses that would meet these criteria. The glasses were designed only for calibration of the Stokes shifted side of the Raman spectra and are not useful for broad ranges of anti-Stokes shifted spectra. After evaluating many glass compositions for these characteristics, a ternary glass matrix of 69.5 wt %  $\text{SiO}_2$ , 6.95 wt %  $\text{Na}_2\text{O}$ , and 26.65 wt %  $\text{B}_2\text{O}_3$ , doped with 0.05 wt %  $\text{Cr}_2\text{O}_3$ , was chosen to become SRM 2241 for use with laser excitation at 785 nm.

Standard Reference Materials® 2242 (laser excitation 532 nm) and 2243 (laser excitations of 488 nm and 514.5 nm) are of the same glass composition. This is a borate glass matrix doped with 0.15% by weight of  $\text{MnO}_2$  to provide the luminescent ion. The glass is 69.85 wt %  $\text{B}_2\text{O}_3$  stabilized with 5 wt %  $\text{SiO}_2$ , 5 wt %  $\text{ZnO}$ , and 5 wt %  $\text{Li}_2\text{O}$ .

The  $\text{SiO}_2$  was obtained from Unimin Corporation (New Canaan, CT) as high purity crystalline quartz, specified with low iron and  $\text{Al}_2\text{O}_3$ . The oxide of sodium was added as the

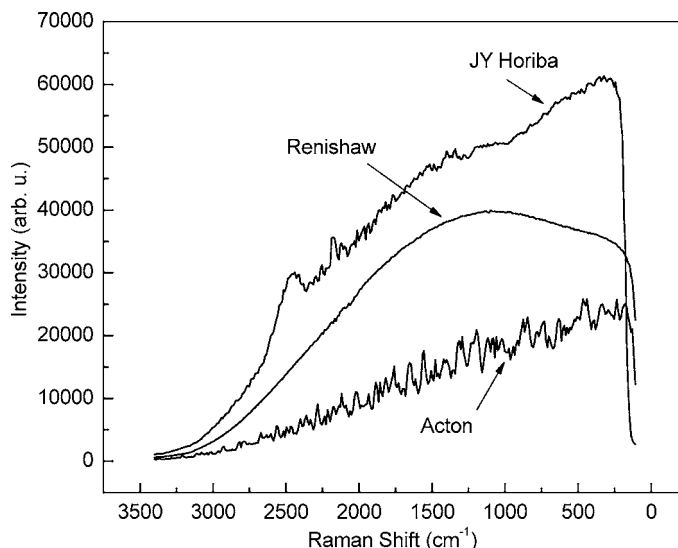


Fig. 3. Intensity-uncorrected spectra of the calibrated irradiance source acquired with the three spectrometers used in the certification measurements.

reagent grade carbonate ( $\text{Na}_2\text{CO}_3$ ) and obtained from Mallinckrodt Baker (Phillipsburg, NJ). The boric anhydride used was laboratory grade obtained from Fisher Scientific (Fair Lawn, NJ). Chromium was added as the oxide ( $\text{Cr}_2\text{O}_3$ ) and was a certified laboratory reagent from Fisher Scientific. The oxide of lithium was added as the reagent grade carbonate ( $\text{Li}_2\text{CO}_3$ ) and obtained from Mallinckrodt Baker.  $\text{MnO}_2$  was added as the oxide and was a certified laboratory reagent from Fisher Scientific.

The glass melts for each SRM were prepared in two kilogram sized batches to ensure homogeneity of both the chemical and resulting optical properties. The reagents were weighed, mixed in the correct proportions, and then melted in a platinum crucible. The mixture was heated to  $1415\text{ }^\circ\text{C}$  and stirred at this temperature for 4.5 hours to allow complete mixing and conversion of carbonates to oxides. The glass was then cooled and held overnight at  $950\text{ }^\circ\text{C}$ . The melt was then reheated to  $1415\text{ }^\circ\text{C}$  and stirred for an additional 2.5 hours. After stirring, the glass was allowed to cool for 1 hour to  $1375\text{ }^\circ\text{C}$  and then poured into a rectangular mold approximately 25 mm thick. The blocks were then annealed overnight at  $540\text{ }^\circ\text{C}$  and allowed to cool slowly to ambient temperature in the oven.

Each of the blocks was diced into smaller sub-blocks from which seven samples (each approximately 3 mm thick) of the SRM were obtained. For the initial homogeneity study of SRM 2241, five sub-blocks were tested. These sub-blocks came from the corners and center of the larger melt. The location of each of the SRM samples within the sub-blocks was preserved throughout the glass processing. The resulting 35 samples were measured in a random order on the micro-Raman system. Analysis of variance testing of the luminescence spectra failed to reveal any significant sample differences among sub-blocks or within any level of a sub-block. Additional samples from the second block were compared with those of the first block, with the same results. As a result, this SRM was batch certified, i.e., a statistical sampling of each lot was used to determine the final corrected luminescence spectrum of each SRM. Testing of SRM 2242 (and 2243) yielded identical results for the homogeneity of the melt.

Each SRM unit has dimensions of  $10\text{ mm} \times 30\text{ mm} \times 2.3$

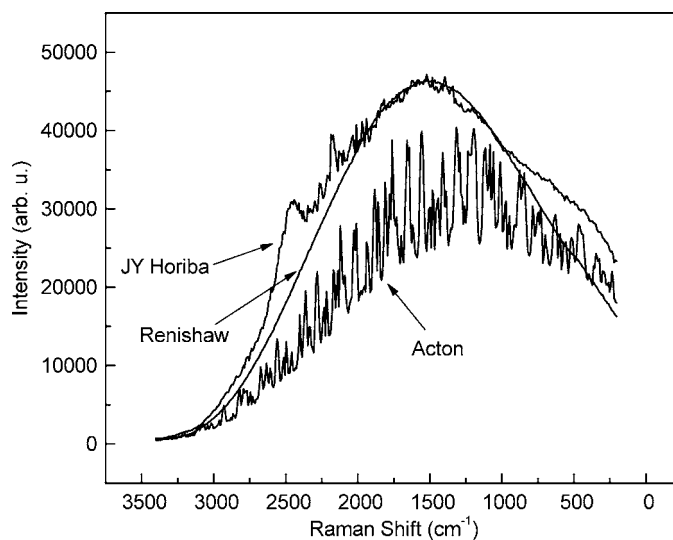


Fig. 4. Intensity-uncorrected SRM 2241 luminescence spectra acquired with the three spectrometers used in the certification measurements.

mm and is mounted into a NIST-designed cuvette type holder. Each unit has one flat optically polished and the opposite flat ground to a frosted finish using a 400 grit polish. All measurements were performed on the frosted surface of the SRM. The finished SRM glass slides are flat to within  $\pm 0.03$  mm, as was crudely established by light microscopy. The average surface roughness of the frosted surface was obtained using surface profilometry to determine the average surface roughness,  $R_a$ , which corresponds to the average peak-to-valley excursions.<sup>15</sup> For SRM 2241,  $R_a$  was  $0.93\text{ }\mu\text{m}$  to  $1.26\text{ }\mu\text{m}$ . For SRMs 2242 and 2243, the average surface roughness was characterized by  $R_a$  values in the range of  $1.31\text{ }\mu\text{m}$  to  $1.49\text{ }\mu\text{m}$ .

**Temperature Studies of Glass Luminescence.** The temperature dependence of the luminescence spectrum of the SRM glass was investigated using an in-house designed and constructed temperature cell. The temperature of the SRM glass was controlled to within approximately  $1\text{ }^\circ\text{C}$  using this apparatus, and the range of temperatures studied was from  $10\text{ }^\circ\text{C}$  to  $70\text{ }^\circ\text{C}$ . The luminescence data were collected with the Renishaw micro-Raman system using the  $10\times$  microscope objective.

## RESULTS AND DISCUSSION

**Certification of Standard Reference Material® 2241.** Standard Reference Material® 2241, certified for laser excitation of  $785\text{ nm}$ , was the first reference material of the series to be developed. Uncorrected spectra of one of the white-light sources obtained with each of the three spectrometers discussed previously are shown in Fig. 3. The corresponding uncorrected luminescence spectrum of SRM 2241, acquired under the same measurement conditions, is shown in Fig. 4. As can be seen in both Fig. 3 ( $\text{LS}_1$ ) and Fig. 4 (SRM 2241), structured etaloning was a major contributor to the system response correction for the Acton and JY Horiba spectra. Figure 5 shows the corresponding intensity-corrected SRM 2241 spectra acquired by each of the spectrometers shown in Figs. 3 and 4 as calculated by Eq. 3. The corrected luminescence spectra are essentially featureless with a band maximum centered at approximately  $2250\text{ cm}^{-1}$ . It is noted that the effects of etaloning were removed, since in these

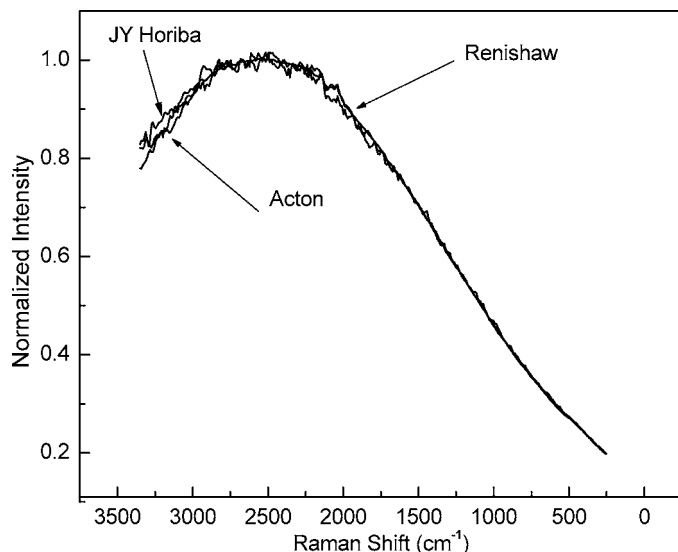


FIG. 5. SRM 2241 relative intensity-corrected luminescence spectra obtained with the three spectrometers used in the certification measurements. Units of the normalized y-axis are photons  $s^{-1} (cm^{-2})(cm^{-1})^{-1}$ .

measurements the grating positions were carefully reproduced between the white light and luminescence measurements. The luminescence spectra have good spectral intensity over the entire Raman spectral region (i.e.,  $100\text{ cm}^{-1}$  to  $3600\text{ cm}^{-1}$ ). As the glass was determined to be optically homogeneous, a batch certification protocol was designed.

**Standard Reference Material® 2241 Corrected Luminescence Spectrum and Polynomial Determination.** A set of 23 intensity-corrected spectra of the 2241 glass was obtained by varying the instrument and collection parameters of the three spectrometers. The temperature of the SRM glass and the wavelength of excitation were not varied in obtaining these spectra. All spectra were acquired over the range of  $3600\text{ cm}^{-1}$  to  $100\text{ cm}^{-1}$  Raman shift ( $785\text{ nm}$  excitation); however, the decrease in detector sensitivity for the Renishaw system above

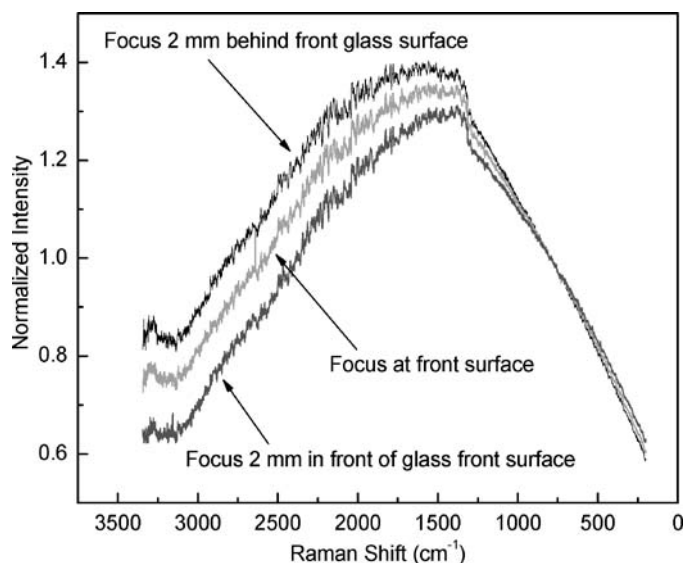


FIG. 6. Effect of the collection lens focus position on the luminescence spectrum of a doubly polished candidate SRM chromium glass.

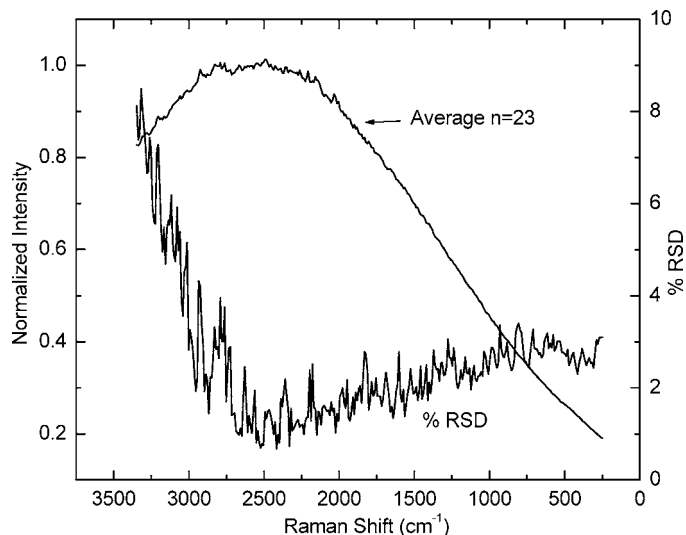


FIG. 7. Average and percent relative standard deviation (%RSD) for the set of SRM 2242 spectra submitted for certification.

approximately  $3500\text{ cm}^{-1}$  and the holographic notch filter spectral edge effects below  $200\text{ cm}^{-1}$  for the JY Horiba/Acton data limited the practical spectral range to  $3400\text{ cm}^{-1}$  to  $200\text{ cm}^{-1}$ . The spectra obtained with the three spectrometers varied in data density, and all the spectra were forced to the same data point spacing using the Grams/32 interpolation routine (Interpol.ab). The resulting data point spacing was approximately  $1\text{ cm}^{-1}$ . However, because the luminescence of this glass is very broad, the spectral data set for the polynomial determination was reduced to  $10\text{ cm}^{-1}$  data point spacing using a ten-point moving-window-average routine (DERES.ab) provided in the Grams/32 software.

For the measurements obtained with the macro-Raman systems, the shape of the luminescence spectrum was observed to be dependent upon the focus position of the collection lens relative to the front surface of the glass. The effect was large if the glass had doubly polished surfaces, as illustrated in Fig. 6 where the change in the collection lens focus position was  $\pm 2\text{ mm}$ . This effect was observed for both thick ( $>10\text{ mm}$ ) and thin ( $<1\text{ mm}$ ) samples. These complications are remedied by frosting the surface of the glass, and the spectral shape then becomes invariant with these sample translations. As a result, for the macro-Raman systems, the position on the sample stage of the focus point was carefully determined, and all spectral data were taken using the frosted surface of the glass at this position.

In Fig. 7 are shown the average and the relative standard deviation (RSD) spectral curves obtained from the set of spectra that were used to determine the coefficients of the polynomial describing the corrected luminescence of SRM 2241. The variability of the RSD spectrum is within 5% of the mean spectrum, except for the extreme spectral ranges. The variability of the data above  $3200\text{ cm}^{-1}$  is due to the lower detection efficiency of the silicon array detectors. The variability below  $1000\text{ cm}^{-1}$  is due to the normalization of all the curves at  $2500\text{ cm}^{-1}$ . The small differences in shape between the data sets therefore results in increasing deviations from the average shape with distance from the normalization point.

Given the limitations of photon sensitivity of CCDs above

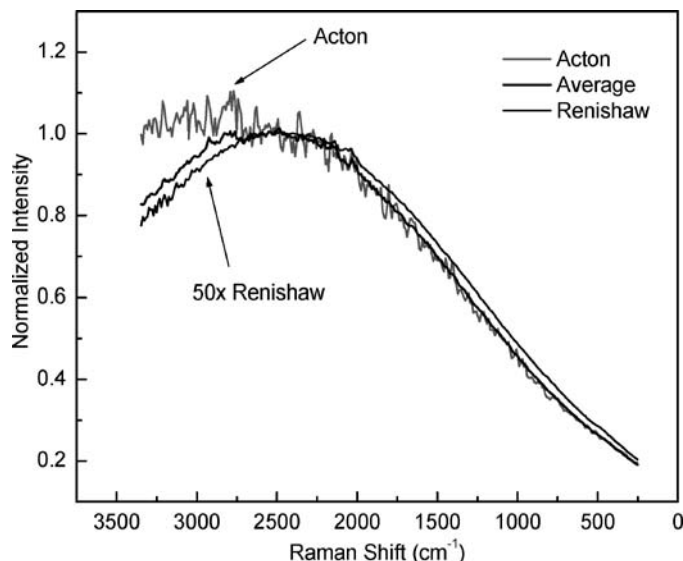


FIG. 8. Variation of spectral shape of SRM 2241 with collimated laser (macro-Raman) and focused laser (micro-Raman) excitation of the luminescence. The average of the data set of 23 certification spectra are included for comparison.

1065 nm ( $\sim 3350 \text{ cm}^{-1}$  Raman shift), the entire luminescence curve of SRM 2241 cannot be completely determined with our instrumentation. For the purposes of certification, the shape of the luminescence spectrum above  $3400 \text{ cm}^{-1}$  cannot be inferred. Therefore, a polynomial expression rather than a more spectroscopically relevant model was used to fit the incomplete shape of the intensity-corrected luminescence curve.

Our analysis of the data found only one systematic effect that was correlated with the variance of the data. Several spectral data sets of SRM 2241 were collected on the JY Horiba and Acton with an unfocused, collimated laser beam. This is a configuration that is almost never utilized in practice but it represents one limit for the illumination of the sample and consequent spectral collection (in  $180^\circ$  backscatter mode). The other limit, i.e., vanishingly small focal length/infinite magnification, is unobtainable, but can be approximated with a  $50\times$  (NA 0.65) microscope objective (working distance of  $\sim 300 \mu\text{m}$ ) as used with the micro-Raman system. Figure 8 shows the average of the 23 spectra in the certification set compared to an unfocused laser spectrum collected with a macro-Raman system and a spectrum collected on the micro-Raman system with a  $50\times$  microscope objective. Clearly, there is a systematic difference in the higher wavenumber region between the unfocused and very tightly focused illumination and collection geometries. The cause of this effect is not well understood, but for the  $50\times$  measurements is likely due to overfilling of the microscope objective. Only the  $10\times$  and  $20\times$  data from the Renishaw were used for the certification. However, to increase the robustness of the certified polynomial fit, the unfocused data for the Acton and JY Horiba were included. The inclusion of these data increases the uncertainty of the shape of the luminescence beyond  $3000 \text{ cm}^{-1}$  and is reflected in the increased RSD of the curve above this spectral region.

Polynomials of several orders were fit to the certification data set and a quintic expression was found to provide the lowest and least structured residuals. The certified polynomial coefficients describing the average intensity-corrected SRM

TABLE I. Coefficients of the certified Polynomial and of the confidence curves describing the luminescence spectrum of SRM 2241 (valid for temperatures of  $20^\circ\text{C}$  to  $25^\circ\text{C}$ ).

Polynomial coefficient	Certified value polynomial coefficient <sup>a</sup>	Polynomial coefficient <sup>a</sup> of the $\pm 2\sigma$ confidence curves	
	$20^\circ\text{C}$ to $25^\circ\text{C}$	+95% CC, ( $+2\sigma$ )	-95% CC, ( $-2\sigma$ )
$A_0$	$1.3535 \times 10^{-01}$	$1.4221 \times 10^{-01}$	$1.2916 \times 10^{-01}$
$A_1$	$2.1658 \times 10^{-04}$	$2.2349 \times 10^{-04}$	$2.1016 \times 10^{-04}$
$A_2^b$	0	0	0
$A_3$	$1.8936 \times 10^{-10}$	$1.9434 \times 10^{-10}$	$1.8034 \times 10^{-10}$
$A_4$	$-9.837 \times 10^{-14}$	$-1.0331 \times 10^{-13}$	$-9.099 \times 10^{-14}$
$A_5$	$1.2414 \times 10^{-17}$	$1.3532 \times 10^{-17}$	$1.0948 \times 10^{-17}$

<sup>a</sup> Where  $I_{\text{SRM}}(\Delta\nu) = A_0 + A_1(\Delta\nu)^1 + A_2(\Delta\nu)^2 + A_3(\Delta\nu)^3 + A_4(\Delta\nu)^4 + A_5(\Delta\nu)^5$ ; for  $\Delta\nu = 225 \text{ cm}^{-1}$  to  $3350 \text{ cm}^{-1}$  and  $\Delta\nu$  is the wavenumber expressed in the units of Raman shift ( $\text{cm}^{-1}$ ).

<sup>b</sup> Regression analysis yields a  $\Delta\nu^2$  term with a t-statistic of absolute value less than 2 (coefficient statistically indistinguishable from zero).

2241 luminescence were determined by calculating the linear least squares fit<sup>16,‡</sup> to the entire SRM data set (all 23 curves), rather than the mean of this data set. The two approaches produce equivalent results only if each data set has the same spectral range. Several of the included data sets were truncated; thus, the global fit was more appropriate. When the data were modeled with the full fifth-order fit, the second-order coefficient was statistically insignificant, i.e., the absolute value of the associated t-statistic was less than 2. Therefore, this term was eliminated, and the data refitted, less the second-order term. The resulting coefficients for this fit are listed in Table I. The resulting coefficients are significant to six places, which must be used for accurate calculation of the certified shape of this SRM. Calculation of intensity correction values above the certified value of  $3350 \text{ cm}^{-1}$  or below  $225 \text{ cm}^{-1}$  Raman shift will result in erroneous results.

Also listed in Table I are the polynomial expressions describing the  $2\sigma$  estimates of the total error about the mean ordinate curve derived using a Type B on Bias (BOB) analysis.<sup>17</sup> Rather than use a t-interval, a BOB estimate is warranted when a small number of reference measurement methods are used and unknown, but sources of systematic uncertainty are present. A t-statistic assumes a number of reference methods with bias centered at zero. In addition, for small numbers of  $n$  (methods) the  $t_{n-1,95}$  is perhaps unreasonably large. The 95% confidence curves derived from the BOB analysis approximate the uncertainties of the fifth-order fit, making use of both the inter- and intra-instrument scatter. The results of this calculation are *not* the polynomial coefficients listed in Table I, but rather a table of the BOB estimates for each data point (wavenumber) in the corrected spectrum. While this is rigorous, it is not readily usable by an end user of the SRM. A smooth polynomial fit to the general trend is sufficient to describe the error bounds of the instrumental scatter around the fifth-order polynomial. The corrected shape of SRM 2241 (and the confidence limits) is calculated as:

$$I_{\text{SRM}}(\Delta\nu) = A_0 + A_1 \times (\Delta\nu)^1 + A_2 \times (\Delta\nu)^2 + A_3 \times (\Delta\nu)^3 + A_4 \times (\Delta\nu)^4 + A_5 \times (\Delta\nu)^5 \quad (4)$$

<sup>‡</sup> Dataplot is a free, public-domain, multi-platform software system for scientific visualization, statistical analysis, and nonlinear modeling.

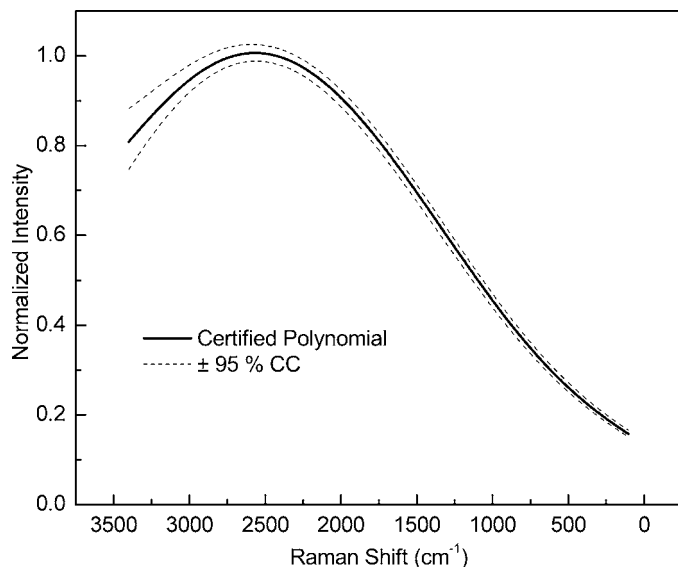


FIG. 9. SRM 2241 spectrum calculated from the certified polynomial with 95% confidence curves.

where  $(\Delta\nu)$  is the wavenumber in units of Raman shift ( $\text{cm}^{-1}$ ) and the  $A_n$ 's are the appropriate coefficients listed in Table I. The corrected shape,  $I_{\text{SRM}}(\nu)$ , has been normalized to unity and is a relative unit expressed in terms of photons  $\text{s}^{-1} \text{cm}^{-2} (\text{cm}^{-1})^{-1}$ .  $I_{\text{SRM}}(\Delta\nu)$  and its associated 95% confidence curves (CC) are shown in Fig. 9. There are three general segments of the error curve. From  $255 \text{ cm}^{-1}$  to approximately  $1300 \text{ cm}^{-1}$ , the BOB  $2\sigma$  uncertainty is approximately 3% to 4%. From  $1300 \text{ cm}^{-1}$  to  $2900 \text{ cm}^{-1}$  the BOB  $2\sigma$  uncertainty is approximately 2%, while from  $2900 \text{ cm}^{-1}$  to  $3350 \text{ cm}^{-1}$  it rises to 6% to 8%.

**Procedure for Obtaining an Intensity-Corrected Raman Spectrum.** The procedure for relative-intensity correcting a measured Raman spectrum,  $S_{\text{MEAS}}(\Delta\nu)$ , requires that the measured luminescence of the SRM,  $S_{\text{SRM}}(\Delta\nu)$ , be determined at the same data point spacing as  $S_{\text{MEAS}}(\Delta\nu)$ . The elements of  $I_{\text{SRM}}(\Delta\nu)$  are obtained by evaluating Eq. 4 at this same data-point spacing, and the spectral intensity correction curve is then:

$$C_{\text{SRM}}(\Delta\nu) = I_{\text{SRM}}(\Delta\nu)/S_{\text{SRM}}(\Delta\nu) \quad (5)$$

The relative intensity-corrected Raman spectrum  $S_{\text{CORR}}(\Delta\nu)$  is then:

$$S_{\text{CORR}}(\Delta\nu) = C_{\text{SRM}}(\Delta\nu) \times S_{\text{MEAS}}(\Delta\nu) \quad (6)$$

#### Photostability of Standard Reference Material® 2241.

The photostability of SRM 2241 was assessed by illuminating samples of the SRM with 140 mW of 785 nm laser light through a 20× (NA 0.40) microscope objective lens. As the theoretical spot size using this objective is approximately  $4 \mu\text{m}$ , the laser power density at the sample could potentially approach  $1 \text{ MW}/\text{cm}^2$ . Thirty spectra were acquired at two-minute intervals for a total illumination time of approximately 1.5 hours. No observable decrease of the sample luminescence signal was observed during this time period. The average of the spectra had a calculated relative standard deviation (RSD) of less than 0.5% over the entire spectrum, which was attributed

to laser power fluctuations. Neither photobleaching nor sample heating was evident during this duration of sample illumination. Laser irradiances of this magnitude are well outside the range that one would employ in the normal use of this SRM.

**Dependence of the Glass Luminescence on the Excitation Wavelength.** The variation of the luminescent response of SRM 2241 with changes in the wavelength of laser excitation was determined using the JY Horiba spectrometer and the tunable Ti:S laser. Measurements were made with laser excitations of 780 nm to 788 nm in 2 nm increments. The angle of the 785 nm notch filter was adjusted with each change of excitation wavelength to minimize the Rayleigh scattered light. A white-light  $\text{LS}_x$  spectrum was acquired at each angle of the notch filter to correct for any differences in its transmission. The intensity-corrected luminescent response with changing laser wavelength excitation for the  $x$ -axis in Raman shift units ( $\text{cm}^{-1}$ ) was found to be invariant with the laser excitation wavelength over this 8 nm range. The intensity-corrected luminescent response with changing laser wavelength for the  $x$ -axis in wavelength units (nm) changes only slightly, with the peak of the curve shifting to longer wavelengths as the laser wavelength increases. If it is desired to use this SRM for calibration of spectrometer systems in the unit of wavelength, the appendix of the certificate for SRM 2241 contains the appropriate coordinate axis transformation equation.<sup>10</sup>

The changes that are observed in the shape of the glass luminescence spectrum on the wavelength scale are of the same magnitude as the experimental variability that is observed in the measurement of fluorescent glasses at 785 nm for the various sampling geometries. For laser excitation between 784 nm and 786 nm, modeling demonstrates that the effect of changing the laser wavelength will result in a change of spectral shape that does not exceed 2%. For laser excitation between 782 nm and 788 nm, modeling shows that the effect of changing the laser wavelength will result in spectral shape changes that are within the 95% confidence intervals of certified corrected luminescence. By expressing the shape of the luminescence response in terms of Raman shift in the intensity response correction algorithm, no correction is needed for differences in the laser wavelength for laser excitations that vary from 784 to 786 nm.

#### Dependence of Glass Luminescence on Temperature.

The  $\text{Cr}^{3+}$ -doped glasses have been studied in the near-infrared region as potentially tunable laser glasses.<sup>18,19</sup> Chromium ( $\text{Cr}^{3+}$ ), as an optically active ion, enters the glass as a network former on account of its size and valence state. Typically, in aluminosilicate glasses,  $\text{Cr}^{3+}$  resides in octahedral sites, especially in the presence of sodium ions.<sup>18</sup> Two absorption bands are observed for the glass in the region 250 nm to 850 nm, and it is because of these features that broadband luminescence of  $\text{Cr}^{3+}$  is expected from a  ${}^4\text{T}_2$  to  ${}^4\text{A}_2$  transition. This broadband luminescence consists of an intense band that peaks at approximately 895 nm (at room temperature) when excited with 785 nm radiation. This luminescence band is characterized by a fairly pronounced temperature dependence showing a bathochromic (red) shift of about 30 nm for a temperature drop of 100 degrees (from 300 K to 200 K).

The uncorrected luminescence spectra of SRM 2241 (Fig. 10) demonstrate an overall reduction in luminescence intensity as well as a shift in the luminescence peak maximum to values closer to the excitation wavelength with increasing temperature. The peak shift is approximately linear with temperature

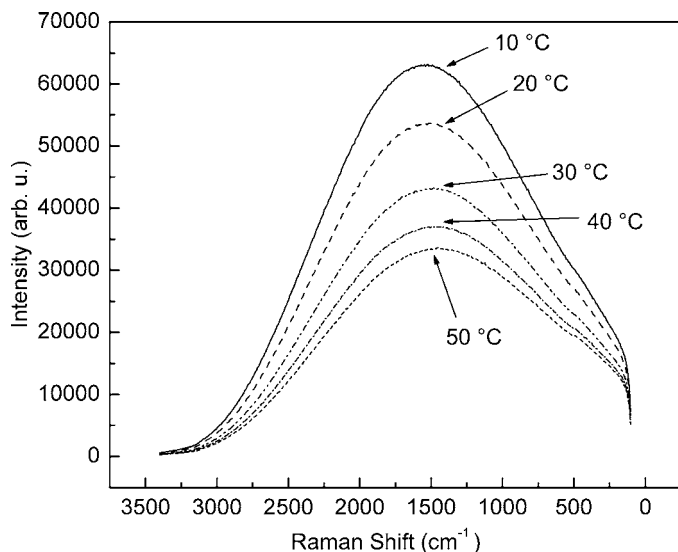


FIG. 10. Intensity-uncorrected spectra of SRM 2241 as a function of temperature.

with a slope of approximately  $-1.5 \text{ cm}^{-1}/^{\circ}\text{C}$  and an intercept of  $1585 \text{ cm}^{-1}$ . The peak shape also broadens asymmetrically (towards low Raman shift) as the temperature increases. This temperature dependence has been observed in other Cr glass systems and is consistent with the results from Ref. 18.

The polynomial coefficients determined for the corrected shape of SRM 2241 utilized data that were obtained at room temperature that was stable to  $23 \text{ }^{\circ}\text{C} \pm 0.5 \text{ }^{\circ}\text{C}$  but controlled only by the room air handling system. The BOB  $2\sigma$  error limits include this uncertainty due to our lack of knowledge of the exact temperature of the SRM at the time of measurement. Although as shown in Fig. 10, changes in the luminescence shape occur with temperature, temperature studies conclude

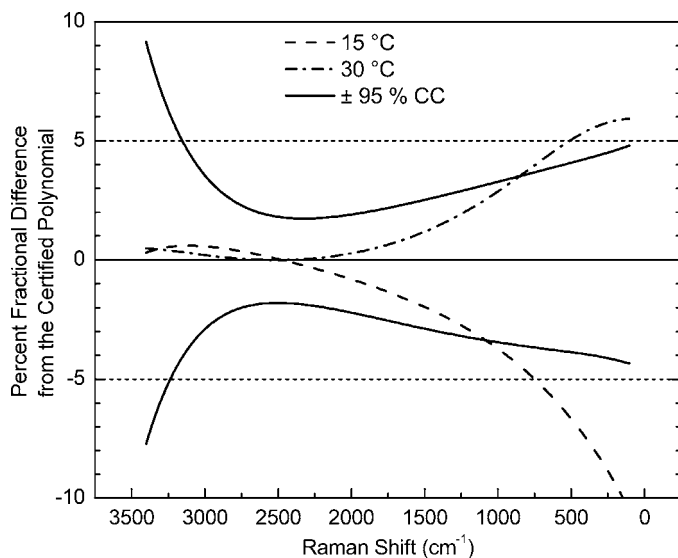


FIG. 11. Relative 95% confidence curves (CC) describing the luminescence spectra of SRM 2241 for 785 nm excitation. The two solid curves represent for SRM 2241 at room temperature, respectively, the percent fractional difference  $(95\% \text{ CC} - I_{\text{SRM}(\Delta\nu)})/I_{\text{SRM}(\Delta\nu)}$ . The dashed curves represent the percent fractional difference between the spectral curves describing the luminescence of SRM 2241 at 15 °C and 30 °C and the reference polynomial.

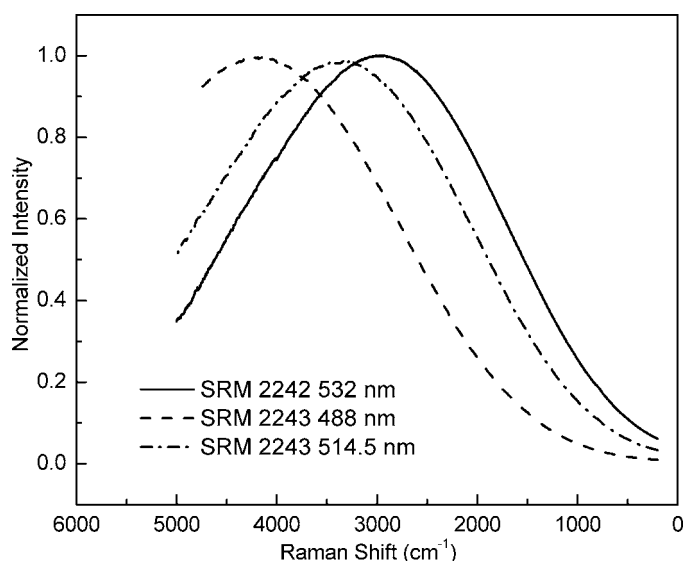


FIG. 12. Spectra of SRM 2242 (532 nm) and SRM 2243 (488 nm and 514.5 nm) calculated from the certified polynomials. Units of the normalized y-axis are photons  $\text{s}^{-1} (\text{cm}^{-2}) (\text{cm}^{-1})^{-1}$ .

that the fifth-order polynomial can accommodate and adequately describe operation of the SRM over a temperature range of  $20 \text{ }^{\circ}\text{C}$  to  $25 \text{ }^{\circ}\text{C}$  and still remain within the stated uncertainties. Operation at temperatures significantly different from room temperature requires use of a separate polynomial expression. These were determined, and the polynomial coefficients for the use of SRM 2241 at  $15 \text{ }^{\circ}\text{C}$  and  $30 \text{ }^{\circ}\text{C}$  operation are also listed in the certificate for SRM 2241.<sup>10</sup> The solid black lines in Fig. 11 show the percent fractional difference, i.e.,  $(95\% \text{ CC} - I_{\text{SRM}(\Delta\nu)})/I_{\text{SRM}(\Delta\nu)}$ , between the 95% confidence curves (CCs) and the certified polynomial for use of the SRM between  $20 \text{ }^{\circ}\text{C}$  and  $25 \text{ }^{\circ}\text{C}$ . The dashed lines show the percent fractional difference between the  $15 \text{ }^{\circ}\text{C}$  and  $30 \text{ }^{\circ}\text{C}$  calculated luminescence spectra and the certified polynomial. Because these dashed lines fall mostly within the 95% CCs for the certified polynomial at room temperature, for all but the most exacting work, the certified polynomial will describe the validity of the SRM from  $15 \text{ }^{\circ}\text{C}$  to  $30 \text{ }^{\circ}\text{C}$ . For operation of the SRM at these extended temperatures, the polynomial functions are conservatively estimated to possess the same uncertainties as the certified room-temperature polynomial for SRM 2241.

**Relative Intensity Correction with Standard Reference Materials® 2242 and 2243.** The certified shapes of the luminescence spectra of SRM 2242 and 2243 when excited with 532 nm, 488 nm, or 514.5 nm laser excitation were determined in a similar fashion as SRM 2241. Experiments were designed to measure the corrected spectrum of the glass on a number of instrument configurations, sampling options, temperatures, and excitation wavelengths to minimize systematic errors.

In Fig. 12 are shown the average corrected luminescence spectra of SRM 2242 and SRM 2243. In contrast to SRM 2241 the certified spectral range of 2242 is  $150 \text{ cm}^{-1}$  to  $4000 \text{ cm}^{-1}$  and for SRM 2243,  $200 \text{ cm}^{-1}$  to  $4800 \text{ cm}^{-1}$ . Both excitation wavelength and temperature were studied as variables to determine the effect on the corrected luminescence shape of each SRM.

Standard Reference Material® 2243 is excited by either the

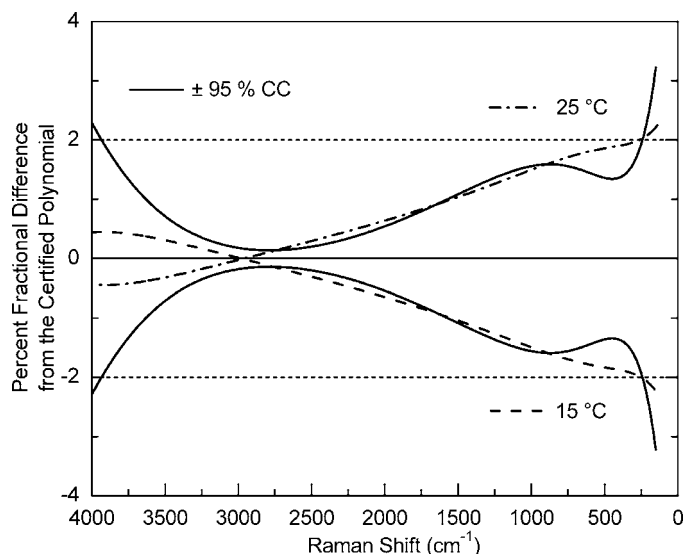


FIG. 13. Relative 95% confidence curves (CC) describing the luminescence spectrum of SRM 2242 for 532 nm excitation. The two solid curves show the percent fractional difference between the  $\pm 95\%$  CC spectral curves and the certified polynomial for 532 nm excitation. The dashed curves represent the percent fractional difference between the spectral curves describing the luminescence spectra of SRM 2242 at 15 °C and 25 °C and the reference polynomial.

488 nm or 514.5 nm laser line of an  $\text{Ar}^+$  laser. Because these are due to atomic line transitions, these excitation wavelengths, for the purposes of this certification, are considered invariant. SRM 2242 is used with 532 nm excitation, which is obtained from doubling the 1064 nm transition found in Nd:YAG or Nd:VO4 lasers. The uncorrected luminescence spectrum of SRM 2242 was found to be invariant with excitation wavelengths between 531 nm and 533 nm as measured with a commercial fluorescence spectrometer. A 2 nm span of excitation wavelengths was considered adequate to cover the range of potential wavelength variation for these common laser systems.

Temperature effects on the spectra of SRM 2242 and 2243 were also evaluated over the range from 5 °C to 60 °C. Unlike SRM 2241, SRM 2243, with either excitation wavelength, showed no shape dependence with temperature. SRM 2242 shows a modest change in the peak location, which can be modeled with the linear relation

$$\text{Peak location of SRM2242}(T) = (-1.9 \text{ cm}^{-1}/\text{°C})T + 2902.26 \text{ cm}^{-1}$$

For the certification of SRM 2242, 66 corrected spectra from the three spectrometer systems were utilized to determine the polynomial and the confidence intervals. The data set includes spectra spanning a temperature range of 20 °C to 25 °C. In contrast to SRM 2241, where the %RSD of the corrected spectra (Fig. 7) ranged as high as 8%, the range for SRM 2242 was between 2% to 3% from 200  $\text{cm}^{-1}$  to 4000  $\text{cm}^{-1}$  Raman shift. This is due to the higher efficiency of the CCDs and holographic gratings used in this spectral range (532 nm to 676 nm). Similarly, for SRM 2243 the 30 spectra utilized for the calculation of the confidence intervals and polynomial expression for both 488 nm and 514.5 nm excitation were less than 3% over the entire certified Raman shift region.

The certified shape of each SRM spectrum was modeled

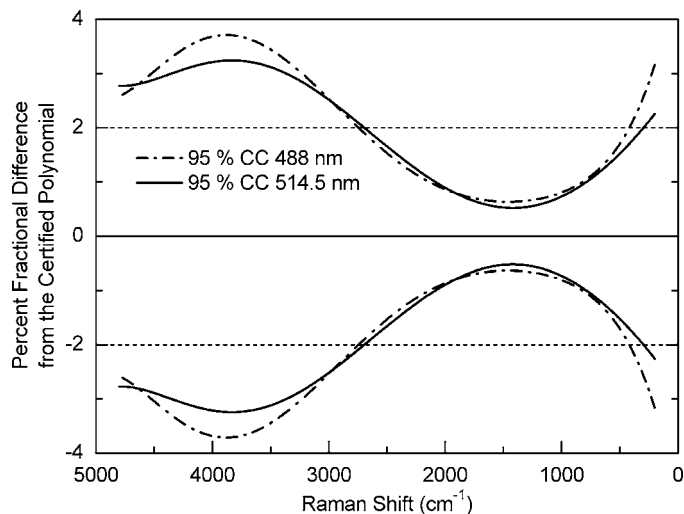


FIG. 14. Relative 95% confidence curves describing the luminescence spectrum of SRM 2243 at room temperature. The two solid black curves show the percent fractional difference between the  $\pm 95\%$  CC spectral curves and the certified polynomial for 514.5 nm excitation. The two dashed curves show the percent fractional difference between the  $\pm 95\%$  CC spectral curves and the certified polynomial for 488 nm excitation. The certified polynomials are valid over the temperature range of 20 °C to 25 °C.

using a polynomial expression and fitted using a least squares analysis as described previously. The certified polynomial coefficients describing corrected luminescence shape and its associated 95% (CC) confidence curves are listed in the appropriate certificate.<sup>10</sup> The confidence curves for SRM 2242, expressed as the percent fractional difference from the certified polynomial, are shown in Fig. 13. The fractional differences of the 95% CCs from the certified polynomial are within 2% for all but the extreme ends of the fit. Although the corrected shape of SRM 2242 is certified for use between 20 °C to 25 °C, with operation between 15 °C and 25 °C the luminescence remains within the bounds of the room temperature 95% CCs. Figure 14 shows the 95% confidence curves for the certified shape of SRM 2243 for both 488 nm and 514.5 nm excitation, again expressed as the percent fractional difference from the certified polynomial.

## VALIDATION OF THE INTENSITY CORRECTION USING MEASURED RAMAN SPECTRA

Once the spectral intensity correction curve for a spectrometer system has been obtained, the determination of the ratios of chosen band areas of a measured Raman spectrum has been suggested as a simple means to provide validation of the intensity correction. Cyclohexane is one of the materials selected as a Raman shift standard by the ASTM Subcommittee on Raman Spectroscopy to check wavenumber calibration of Raman spectrometers, since it has a number of bands that span the Raman shift regions of interest. These same features make cyclohexane a material of interest for intensity validation, and Frost and McCreery have published the peak area ratios for cyclohexane as well as for a number of these Raman shift standards.<sup>7</sup> In addition, extensive measurements of the temperature dependencies of the cyclohexane bands have been reported by Pelletier.<sup>20</sup> For validation using cyclohexane it has

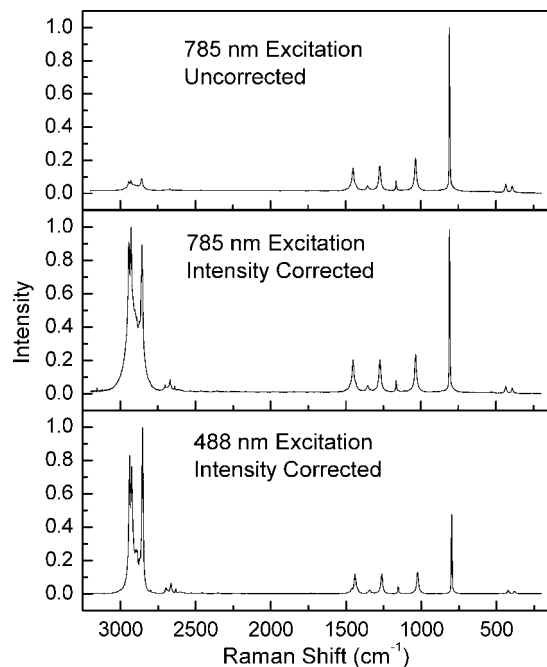


Fig. 15. Raman spectrum of neat cyclohexane with laser excitation of 785 nm. (Top) Uncorrected for spectrometer response, and (middle) corrected with SRM 2241. (Bottom) SRM 2243 corrected spectrum of cyclohexane with laser excitation of 488 nm.

been customary to select the five prominent bands and ratio four of them to the area of the  $802\text{ cm}^{-1}$  band.

The top two panels of Fig. 15 show an uncorrected and a relative intensity-corrected Raman spectrum of cyclohexane obtained with the JY Horiba spectrometer using laser excitation at 785 nm. Significant correction, i.e., correction factors that for this spectrometer range from 4.4 to 31, is required in the C–H stretch region of the spectrum. This correction is also exhibited in Fig. 2, where, for 785 nm excitation, the correction factor that is shown is 10 to 150 times larger in the  $2800\text{ cm}^{-1}$  to  $3500\text{ cm}^{-1}$  region than in the  $800\text{ cm}^{-1}$  region. The relative shapes of intensity-corrected spectra will depend on the laser excitation wavelength, as illustrated in the bottom panel of Fig. 15, which shows the relative intensity-corrected spectrum of cyclohexane at 488 nm. With 488 nm excitation, the spectral shape changes that result from intensity correction are much less than that exhibited in the top panels (see Fig. 2).

These large correction factors can lead to considerable variability of the band area ratios between instruments, as was demonstrated in a multi-lab study utilizing SRM 2241 to correct cyclohexane Raman spectra.<sup>21,22</sup> Initial results obtained in our lab using the micro-Raman system (within instrument) also demonstrated a significant dependence of the final band area ratios on the focus position of the sample, even with low NA collection lenses. A systematic bias that was identified when obtaining data with micro-Raman systems was that the operator typically determined the optimal focus by maximizing the signal intensity obtained from the  $802\text{ cm}^{-1}$  band of cyclohexane and then used this focus position to obtain the entire spectrum. This practice yielded results for the ratio of the all-CH band ( $2587\text{ cm}^{-1}$  to  $3068\text{ cm}^{-1}$ ) to the  $802\text{ cm}^{-1}$  band ( $700\text{ cm}^{-1}$  to  $800\text{ cm}^{-1}$ ) that were invariably lower than if the focus were set to the surface of the sample cell.

A systematic study of band area ratios was done with the JY

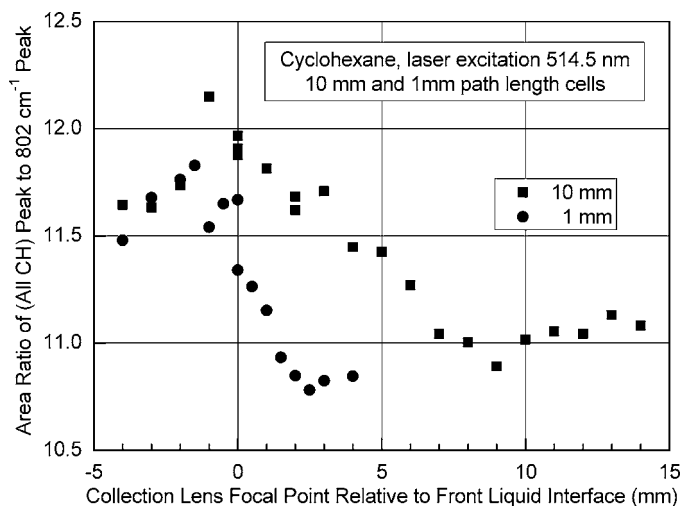


Fig. 16. Area ratio of (all-CH) band to  $802\text{ cm}^{-1}$  band of cyclohexane with laser excitation at 514.5 nm in 10 mm and 1 mm path length cells, as collection lens focal point is varied. Negative values of the  $x$ -axis mean the collection lens focus is in front of the front cyclohexane/window interface of the cell.

Horiba macro-Raman system. In this study it was noted that if the cyclohexane is contained in a typical quartz cuvette, a small but significant quartz Raman band in this same spectral region complicates the spectrum. Additional variability results from obtaining a background signal that corrects for this Raman quartz band. To improve repeatability, we constructed 1 mm and 10 mm path length stainless steel cells with 1 mm thick, 25 mm diameter laser-quality sapphire windows that give negligible Raman interference at  $802\text{ cm}^{-1}$  and also exhibit negligible fluorescence under laser irradiation. The spectra were corrected for their relative intensity using the uniform sphere white-light sources described earlier. The areas of integration for the cyclohexane peaks are the same as those chosen by Frost and McCreery.<sup>7</sup>

For laser excitation of 514.5 nm, the ratio of the all-CH band to the  $802\text{ cm}^{-1}$  band is shown in Fig. 16 as the 10 mm cell was translated relative to the focal point of the spectrometer collection lens. Raman spectra were obtained by moving the cell at 1 mm increments and, using the liquid interface of the front window of the cell as a reference plane, this cell was moved so that the location of the focal point of the collection lens changed from 4 mm in front of this reference plane (negative distances in Fig. 16) to 14 mm behind this reference plane (positive distances in Fig. 16). The ratio changes from an average of about 12 (focusing in front of the cell) to about 11 as the focus is moved into the liquid in the cell, approximately a 9% change. Also shown are measurements made with the 1 mm path length cell, which displays changes that, within the scatter of repeated measurements, are the same in magnitude as for the 10 mm cell. The other cyclohexane bands ( $1028\text{ cm}^{-1}$ ,  $1267\text{ cm}^{-1}$ , and  $1444\text{ cm}^{-1}$ ) lie closer to  $802\text{ cm}^{-1}$  and while the ratios show similar decreases, the relative changes are very small.

As the excitation wavelength is increased, the change in the area ratios as the cell is translated increase for the various band ratios. Figure 17 shows the change in the (all-CH) band ratio, to  $802\text{ cm}^{-1}$  with laser excitation at 647 nm as a function of distance into the sample cell. Here, the decrease is about 20% with increasing depth of focus. Not shown are the results at 785 nm, which start with an (all-CH) to  $802\text{ cm}^{-1}$  band area ratio of

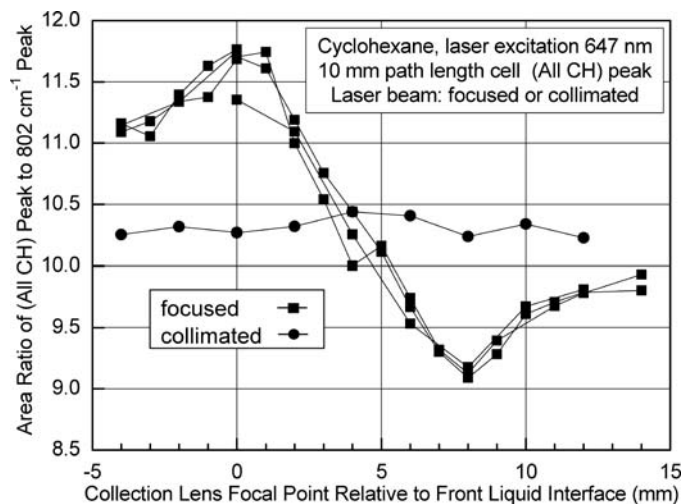


FIG. 17. Area ratio of (all-CH) band to  $802\text{ cm}^{-1}$  band of cyclohexane with  $647\text{ nm}$  laser excitation as either a focused beam or an unfocused (collimated) beam in a  $10\text{ mm}$  path length cell, as the collection lens focal point is varied. The x-axis values are the same as for Fig. 16.

10.5 and drop to 7 with increasing focus depth into the sample cell, a 33% decrease.

These results all derive from using a focused laser beam for the Raman excitation. Figure 17 also shows that the (all-CH) band ratio obtained using an unfocused laser beam (collimated laser light) exhibits no ratio change with cell position. This behavior was observed with measurements at  $785\text{ nm}$  and  $514.5\text{ nm}$ , as well. These results suggest that achromaticity of the collection optics may be partially responsible as position dependence increases at higher excitation wavelengths. Figure 18 shows the (all-CH) to  $802\text{ cm}^{-1}$  area ratio of cyclohexane as a function of collection lens focus position with both a set of visible range achromats and a set of NIR range (design wavelengths of  $706.5\text{ nm}$ ,  $855\text{ nm}$ , and  $1015\text{ nm}$ ) achromats. The substitution of the NIR range achromats reduces the change of the measured area ratios by about 50% for the data collected with  $752\text{ nm}$  excitation.

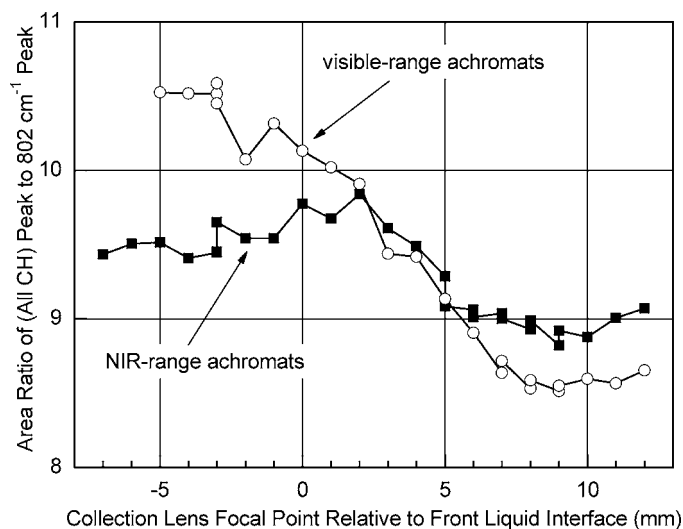


FIG. 18. Area ratio of (all-CH) band to  $802\text{ cm}^{-1}$  band of cyclohexane with  $752\text{ nm}$  laser excitation with visible range and with NIR range achromat collection lenses. The x-axis values are the same as for Fig. 16.

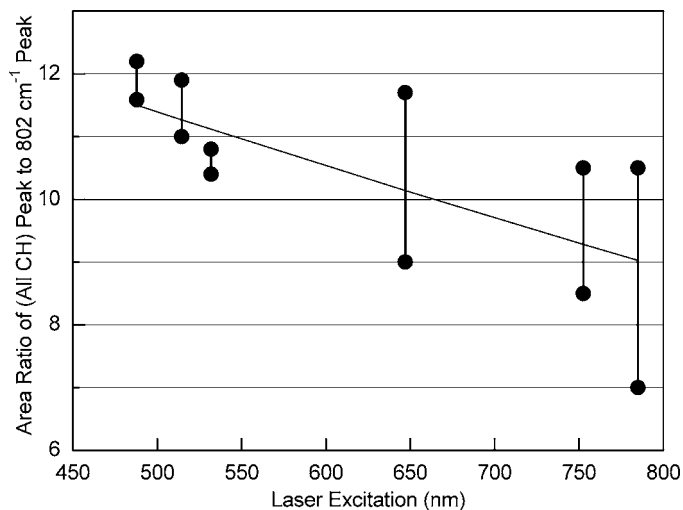


FIG. 19. Area ratio of (all-CH) band to  $802\text{ cm}^{-1}$  band of cyclohexane as a function of laser excitation wavelength. The range of the data at each laser excitation wavelength is a combination of the variation in the measured band area ratios as the collection lens focal point was varied and of an estimate of the data reproducibility. The solid line is a  $v^3$  dependence of these ratios least squares fit to the extremes of these data ranges.

Lastly, for photon-counting detectors such as CCDs, the nonresonant Raman scattering intensity varies as the third power of the absolute wavenumber ( $v^3$ ).<sup>23</sup> Measurements of cyclohexane were made at  $488\text{ nm}$ ,  $514.5\text{ nm}$ ,  $532\text{ nm}$ ,  $647\text{ nm}$ ,  $752\text{ nm}$ , and  $785\text{ nm}$ . Figure 19 displays the range of the (all-CH) peak area ratios at each of these laser wavelengths as the  $10\text{ mm}$  cell position was translated. The line placed on the data is a  $v^3$  dependence least squares fit to the extremes of the range of the data obtained with the visible achromats for each excitation wavelength.

We have not attempted to model the changes in peak area ratio that are observed in these experiments. Several authors have recently modeled the effect of refraction for confocal Raman spectroscopy<sup>24–26</sup> but these have not explicitly discussed effects associated with dispersion in refractive indices of the sample and they are dealing with optics with numerical apertures far larger than those used in the macro-Raman systems.

Currently available data for obtaining Raman spectra of liquids contained in cuvettes are generally not very specific regarding the experimental parameters to be controlled regarding sample positioning and laser parameters. If peak area ratios are to be used as a validation of the intensity correction procedure, these data show that, as a practical matter, considerable thought must be given in the specification of standard practices if consistent and reliable results are to be obtained.

## CONCLUSION

This paper describes three NIST SRMs as certified sources of known relative irradiance for the relative intensity correction of Raman spectra obtained with common excitation laser wavelengths. These SRMs are easily measured in a number of sample configurations including microscope-based systems, and they simplify the measurement process, which can be difficult when employing a calibrated white-light irradiance source. The advantage of these glasses is their ease of use, the

photostability of the luminescence, and their cost relative to a calibrated white-light irradiance source. NIST is currently developing SRM 2244 for the calibration of 1064 nm Raman systems. Measurements of the peak area ratios of cyclohexane can exhibit significant systematic variations that are dependent upon the cuvette placement relative to the collection lens focal point. This result has implications for the development of protocols for the validation of the intensity-correction procedure.

#### ACKNOWLEDGMENTS

The authors wish to thank Professor Richard McCreery of The Ohio State University for many useful discussions and James Maslar of NIST for discussions and help in the laboratory.

1. M. D'Orazio and B. Schrader, *J. Raman Spectrosc.* **2**, 585 (1974).
2. F. J. Purcell, R. Kaminski, and E. Russavage, *Appl. Spectrosc.* **34**, 323 (1980).
3. M. Fryling, C. J. Frank, and R. L. McCreery, *Appl. Spectrosc.* **47**, 1965 (1993).
4. H. Hamaguchi, *Appl. Spectrosc. Rev.* **24**, 134 (1988).
5. M. Malyj and J. E. Griffiths, *Appl. Spectrosc.* **37**, 315 (1983).
6. K. G. Ray and R. L. McCreery, *Appl. Spectrosc.* **51**, 108 (1997).
7. K. J. Frost and R. L. McCreery, *Appl. Spectrosc.* **52**, 1614 (1998).
8. R. L. McCreery, "Raman Spectroscopy for Chemical Analysis", in *Chemical Analysis, A Series of Monographs of Analytical Chemistry and Its Applications*, J. D. Winefordner, Ed. (Wiley-Interscience, New York, 2000), 1st ed., vol. 157, Chap. 10.
9. J. A. Gardecki and M. Maroncelli, *Appl. Spectrosc.* **52**, 1179 (1998).
10. SRM certificates found online: [www.nist.gov/srm](http://www.nist.gov/srm); Standard Reference Material SRM 2241, Relative Intensity Correction Standard for Raman Spectroscopy: 785 nm Excitation (National Institute of Standards and Technology, Gaithersburg, MD).
11. Technology Services, Calibration Program, NIST, Gaithersburg, MD, [www.nist.gov/calibrations](http://www.nist.gov/calibrations).
12. P. Hendra, C. Jones, and G. Warnes, *Fourier Transform Raman Spectroscopy: Instrumentation and Chemical Applications* (Ellis Horwood, New York, 1991).
13. J. Reader, C. H. Corliss, W. L. Wiese, and G. A. Martin, *Wavelengths and Transition Probabilities for Atoms and Atomic Ions*, National Standard References Data Services, National Bureau of Standards (U.S.) **68** (1980); <http://physics.nist.gov/PhysRefData/Handbook/index.html>.
14. "Standard Guide for Raman Shift Standards for Spectrometer Calibration", in *ASTM Annual Book of Standards 2006* (NIST, Gaithersburg, MD, 2006), vol. 3.06, Molecular Spectroscopy, E1840-96.
15. J. F. Wong and T. V. Vorburger, *Appl. Opt.* **30**, 42 (1991).
16. Dataplot, [www.itl.nist.gov/div898/software/dataplot/](http://www.itl.nist.gov/div898/software/dataplot/).
17. N. F. Zhang, D. L. Banks, K. R. Eberhardt, H. K. Liu, M. G. Vangel, M. S. Levenson, J. H. Yen, L. M. Gill, and W. F. Guthrie, *J. NIST Res.* **105**, 571 (2000).
18. D. L. Russell, K. Holliday, M. Grinberg, and D. B. Hollis, *Phys. Rev. B* **59**, 13712 (1999).
19. P. J. Streck, E. Deren, J. Lukowiak, J. Hanuza, H. Drulis, A. Bednarkiewicz, and V. Gaishun, *J. Non-Cryst. Solids* **288**, 56 (2001).
20. M. J. Pelletier, *Appl. Spectrosc.* **53**, 1087 (1999).
21. S. J. Choquette, E. S. Etz, W. S. Hurst, and D. Blackburn, *Am. Pharm. Rev.* **6**, 74 (2003).
22. E. S. Etz, S. J. Choquette, and W. S. Hurst, *Microchim. Acta* **149**, 175 (2005).
23. J. M. Dudik, C. R. Johnson, and S. A. Asher, *J. Chem. Phys.* **82**, 1732 (1985).
24. N. J. Everall, *Appl. Spectrosc.* **54**, 773 (2000).
25. N. J. Everall, *Appl. Spectrosc.* **54**, 1515 (2000).
26. K. J. Baldwin and D. N. Batchelder, *Appl. Spectrosc.* **55**, 517 (2001).